

ADAS Vision Risk Assessment

December 11th, 2022

M.L. Cummings
Benjamin Bauchwitz
Yunseon Kang

Duke University

U.S. DOT Disclaimer

The contents of this report reflect the views of the authors, who are responsible for the facts and the accuracy of the information presented herein. This document is disseminated in the interest of information exchange. The report is funded partially by a grant from the U.S. Department of Transportation's University Transportation Centers Program. However, the U.S. Government assumes no liability for the contents or use thereof.

Acknowledgement of Sponsorship

This project was supported by the Collaborative Sciences Center for Road Safety, www.roadsafety.unc.edu, a U.S. Department of Transportation National University Transportation Center promoting safety.

Contents

- ADAS Vision Risk Assessment _____ 1
 - U.S. DOT Disclaimer 2
 - Acknowledgement of Sponsorship 2
- Introduction _____ 4
- Background _____ 4
- Method _____ 6
 - Highway Test 7
 - Pedestrian Avoidance Test..... 8
 - Data Collection Instruments 12
- Results _____ 14
 - Highway Test 14
 - Pedestrian Avoidance Test 19
 - Automatic Acceleration Events..... 22
- Discussion _____ 23
 - The Highway Test 23
 - The Pedestrian Test..... 23
- Conclusion _____ 24
- References _____ 25
- Appendix A: Car Event Pictures and Sounds _____ 27
- Appendix B: Highway Descriptive Statistics _____ 31
- Appendix C: Pedestrian Descriptive Statistics _____ 34
 - Appendix C.1: Distances to Events 35

Introduction

Vehicles with partial automation, including those with Advanced Driver Assist Systems (ADAS) that leverage embedded artificial intelligence (AI), are increasingly prevalent, but whether they improve overall safety has not been established. The ADAS-equipped vehicles currently deployed require a significant amount of driver supervision and input. Despite impressive improvements in the underlying technology, a stream of recent accidents indicates that these systems may be brittle and continue to suffer from vulnerabilities that are not well understood (NHTSA, 2022b).

Recent research demonstrates that ADAS systems perform inconsistently, and that there can be unexpected significant variability in ADAS performance (AAA, 2022; Cummings & Bauchwitz, 2022; Gross, 2022). These inconsistencies, as well as the overall increase in driving fatalities (NHTSA, 2022a) and pedestrian fatalities (Macek, 2022), indicate more research is needed to determine where possible sources of risk lie for such systems. In addition, several recent studies confirmed that a concerning number of drivers do not understand how their ADAS systems work (J.D. Power, 2022; Mueller, Cicchino, & Calvanelli, 2022).

ADAS systems rely on vision-based lane tracking systems to maintain lateral control (Waykole, Shiwakoti, & Stasinopoulos, 2021), and may combine computer vision with other sensing modalities to maintain space from other vehicles (Kim, Han, & Senouci, 2018; Wei et al., 2020; Ziebinski, Cupek, Grzechca, & Chruszczyk, 2017). However, some vehicles rely exclusively on computer vision for these tasks, without any other sensor redundancy (Tesla, 2021). Sun glare has the potential to be a major issue for such systems, as direct sun can saturate pixel intensities in computer-detected images, making it more difficult to distinguish between the objects in a scene (Ziebinski et al., 2017). Previous research has indicated that the position of the sun could be a factor in whether an ADAS-equipped car correctly implemented driver-alerting logic (Bauchwitz & Cummings, 2022). Therefore, it is especially important to understand the effect of direct sun on automated vehicle control and driver alerting.

Such sensor vulnerabilities raise the concern that autonomous and partially automated vehicles may be at a higher risk for striking pedestrians. For example, a fatal 2018 collision between an experimental Uber self-driving car and a pedestrian was a major setback for the industry (Laris, 2018). While pedestrian detection systems have made important strides in the past decade, recent studies have shown that environmental conditions like darkness can reduce the effectiveness of such systems (Cicchino, 2022). Moreover, pedestrian-centric urban environments have much more road feature diversity than restricted-access highways, which could impair vehicle perception. A previous study suggested that problems with lane markings may negatively influence obstacle detection for an ADAS-equipped vehicle (Cummings & Bauchwitz, 2022). Thus, more work is needed to determine the effect of lane marking quality on pedestrian detection systems for ADAS-equipped vehicles.

With these issues in mind, this study is a follow-on effort from previous Collaborative Sciences Center for Road Safety (CSCRS)-sponsored experiments (Bauchwitz & Cummings, 2022; Cummings & Bauchwitz, 2022) to determine if and to what degree sun glare influences lane keeping and driver monitoring in highway settings for ADAS-equipped vehicles. In addition, this effort examines if and how lane marking quality degrades pedestrian detection.

Background

Lane tracking is a core feature of ADAS and heavily relies on computer vision-based technology. Typically, the most effective lane tracking systems integrate multiple sensor features and include flexible road models that can adapt to a diverse set of environments (Matsushita & Miura, 2011). Many lane tracking systems rely on detecting line segments (Liu, Li, & Huang, 2014; Yuan, Tang, Pan, & Zhang, 2014), though lane tracking systems based on curve detection are becoming more popular because they can handle

more varied road shapes (Wang et al., 2019). Vanishing points are often applied as a constraint because they help resolve ambiguity in visual perspectives (Kong, Audibert, & Ponce, 2009). Lane tracking systems can better perceive contrast at night as compared to humans (Huang & Liu, 2021); however, overall failure rates can approach 10% (Choi, Park, Choi, & Oh, 2012; Yuan et al., 2014).

It is not clear whether and to what degree sun glare contributes to these lane tracking failure rates. Sun glare has been reported to degrade the quality of visual information and lead to incorrect feature extraction (Esfahani & Wang, 2021). Previous research showed a possible relationship between sun position and delays in ADAS-initiated driver takeovers following loss of lane markings (Bauchwitz & Cummings, 2022). Sun glare has been shown in another study to affect visual perception algorithms used in autonomous vehicles, leading to a false positive rate of up to 16% (Yahiaoui, Uricar, Das, & Yogamani, 2020). In situ, unintended disengagements in Tesla Autopilot have been reported as a result of direct sun (Loveday, 2019). Importantly, while these issues are repeatedly raised by users in deployed products, the formal study of the relationship between sun glare and ADAS performance remains limited.

In addition to a possible interaction between sun glare and lane tracking, our previous research looked at how well an ADAS detected obstacles in a construction zone setting, with inconsistent performance results across the same make and model of car (Cummings & Bauchwitz, 2022). Obstacle detection for cars that rely only on computer vision rely heavily on the ability of one or more cameras and the underlying software to recognize an object in their paths, and then to correctly act. Computer vision essentially compares a potential object in the field of view of the cameras to an underlying database of known objects to determine whether the image is an actual obstacle. Then the object is labelled to determine a possible follow-on action.

In this previous research, the obstacle was an orange cone, and in many trials, the car successfully detected and labeled the object but did not take any avoidance actions. In many cases, the cone was not recognized as either a cone or an obstacle. While the consequence of hitting a small orange cone in a controlled test setting was minimal, this raised the question as to how this scenario might have differed if the obstacle resembled a person. Despite recent progress, pedestrian detection systems across different vehicles and settings fail to yield consistent performance.

For example, pedestrian detection systems typically perform more poorly at night, when 75% of pedestrian fatalities occur (Cicchino, 2022; Rajaram, Ohn-Bar, & Trivedi, 2015). Additionally, research has shown that pedestrian detection systems that rely solely on computer vision without other forms of sensor fusion may only eliminate 30% of preventable pedestrian fatalities (Combs, Sandt, Clamann, & McDonald, 2019). Common failure modes include pedestrian occlusion by other objects or when the model is insufficiently trained (Rajaram et al., 2015). Furthermore, recent research suggests that lane detection algorithm performance suffers in complex scenes like those that contain pedestrians (Qiao Huang & Jinlong Liu, 2021). Clearly more work is needed to determine the interaction between lane detection and pedestrian detection, including whether degraded lane lines change pedestrian detection performance.

Lastly, the seriousness of possible lane detection and obstacle detection failures in ADAS-equipped vehicles is directly dependent on whether the human driver is attentive. While drivers are required to be alert and engaged at all times while operating ADAS-equipped vehicles, driver distraction and inattention are increasing in the presence of such systems (Dunn, Dings, & Soccolich, 2019). Despite problems with driver distraction, companies are increasingly advertising hands-free driving capabilities, which means driver monitoring systems need to be especially effective. Unfortunately, our previous study showed that the initiation of driver takeover alerts for ADAS-equipped vehicles was neither consistent within a single car nor across all three of the same makes and models (Bauchwitz & Cummings, 2022). However, this previous work did not look at alert consistency in the presence of sun glare and pedestrians.

The next section outlines the experimental methods for two different experiments designed to address these gaps.

Method

We identified two models of vehicles available through a car-sharing platform for which three or more individual vehicles were consistently available for rental with ADAS capabilities. We chose to focus our sample on Car Model A and Car Model B, both model years of 2021, due to the relatively high levels of availability in the sample region. Tables 1 and 2 provide the technical details for both models. Three cars for both models were selected for testing. The same driver, an experienced test driver, completed all tests. In all experiments, a second experimenter sat in the passenger seat to monitor the status of the recording devices and ensure that cruise control speed was set at the correct level. In track tests, a third experimenter controlled the movement of the pedestrian test target. Make and model information can be provided upon request.

Table 1: Technical details of Car Model A

Feature	Description
Lane Keeping Assist	It detects lane markers on the road with a camera mounted on the front windshield. When the system detects the vehicle straying from its lane, it alerts the driver with a visual and audible warning. The vehicle and lane markings are visualized on a screen inside the vehicle.
Forward Collision Warning (First warning)	This warning message appears on a Liquid-Crystal Display (LCD) with a warning chime and the steering wheel vibrates, and the vehicle may slow down depending on proximity to the obstacle.
Automatic Emergency Braking (Second warning)	The warning message appears on the LCD with a warning chime. Some vehicle system intervention occurs by the engine management system to help decelerate the vehicle.

Table 2: Technical details of Car Model B

Feature	Description
Lane Keeping Assist	It monitors the markers on the driving lane as well as surrounding areas for the presence of vehicles or other objects. The immediate roadway and car are displayed on an LCD. The vehicle and lane markings are visualized on a screen inside the vehicle.
Forward Collision Warning	It provides visual and audible warnings in situations when the vehicle detects that there is a high risk of a frontal collision.
Automatic Emergency Braking	It automatically applies braking to reduce the effect of a frontal collision. When applied, the LCD generates a visual warning, and the system sounds a chime.
Obstacle-Aware Acceleration	Accelerating is adjusted if the vehicle detects an object in its immediate driving path. When an obstacle is encountered the vehicle will decelerate, and when the obstacle moves or is evaded, the vehicle will accelerate back to its previous speed.

Highway Test

The objective of the first test was to determine how sun glare affects driver alerting and unanticipated driver handoffs during semiautomated highway driving. A secondary objective was to characterize variability within a single individual vehicle as well as across vehicles with the same brand of ADAS system. Trials were evaluated for the prevalence of requests for driver steering, unintended driver handovers, phantom braking, and audio/visual alarms.

Each trial consisted of driving the vehicle on a 4.5-mile stretch of east-west highway. The route used is shown in Figure 1 and encompasses a section of the Northern Wake I-540 Expressway between Exit 7 (junction with Leesville Road) and Exit 11 (junction with Six Forks Road). Each of the six vehicles underwent 10 trials in each direction under a high sun angle condition (sun altitude > 40 degrees) and 10 trials in each direction under a low sun angle condition (sun altitude ≥ 4 degrees and < 20 degrees). summarizes the design matrix for this experiment. Given the east/west course, half the trials had the sun

Model	Number of vehicles	Trials per vehicle	Direction	Sun altitude condition
A	3	10	East	Low
	3	10	West	Low
	3	10	East	High
	3	10	West	High
B	3	10	East	Low
	3	10	West	Low
	3	10	East	High
	3	10	West	High

behind the cars, with the other half in front. There were a total of 240 trials, half with a high sun and half with low sun. Experiment timing was dictated by the reservation period for each vehicle, with all low sun angle trials for a vehicle occurring in two 90-minute blocks and all high sun angle trials occurring in a single 180-minute block. The data were collected over a 7-week period in July and August, 2021.

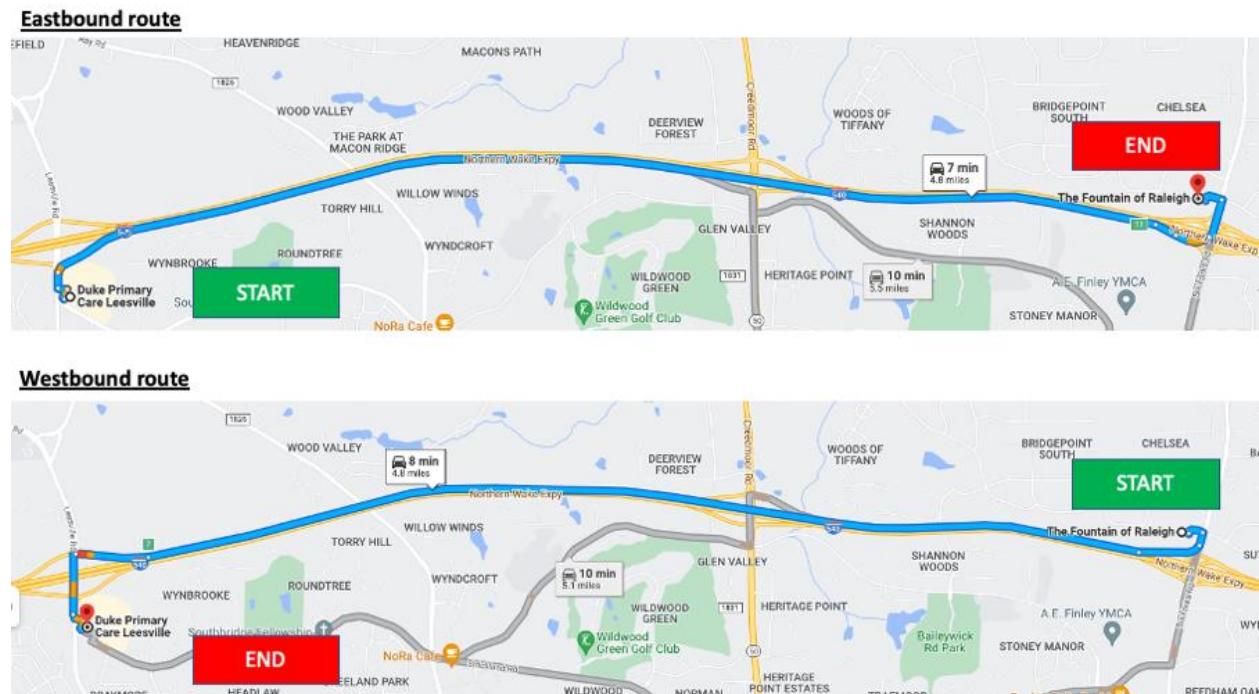


Figure 1: Highway test route

At the beginning of each trial, the vehicle was driven onto the highway and immediately merged into the center lane (second from the left), with adaptive cruise control activated and set to 70 MPH, which is the speed limit for the road. The center lane provided the least disruption from especially slow- or fast-moving traffic. Automatic steering was engaged as soon as the entrance ramp ended and continued until the beginning of the exit ramp at the opposite end of the route. The driver did not engage with any vehicle controls while automatic steering was engaged, except to respond to alerts or if a safety hazard was detected. The ADAS system was reset between each trial at the locations marked start/end in Figure 1.

Both vehicle types presented various alerts to the driver, including requesting that the driver briefly interact with the steering wheel. When this occurred, the driver gently tilted the steering wheel with minimum force and amplitude and let go of the wheel as soon as the hands-on alert terminated. Intended steering amplitude was intended to be 3 degrees \pm 1 degree in either direction. During these interventions, the wheel was held using a standard 10:00/2:00 2-handed grip. If the vehicle initiated a full handover of control, the driver took control and transferred control back to the vehicle as soon as the ADAS and course permitted.

Table 3: Highway test design matrix

Model	Number of vehicles	Trials per vehicle	Direction	Sun altitude condition
A	3	10	East	Low
	3	10	West	Low
	3	10	East	High
	3	10	West	High
B	3	10	East	Low
	3	10	West	Low
	3	10	East	High
	3	10	West	High

Pedestrian Avoidance Test

The objective of this test was to investigate any possible interactions between lane and pedestrian detection, as well as to measure any effect on driver alerting. A secondary objective was to characterize variability within a single individual vehicle as well as across vehicles with the same brand of ADAS. Trials were evaluated for the prevalence and timing of detection and braking as well as the prevalence and timing of any audio/visual alarms.

Each trial consisted of driving one of the six vehicles on a 1,500-foot section of track (Figure 2) at the North Carolina Center for Automotive Research (NCCAR), a closed test track facility. The roadway is 40 feet wide, which was then separated into three 13-foot-wide lanes. All cars experienced regular lane line trials, which were standard 10-foot by 6-inch lines with 30-foot longitudinal spacing, as specified in the Manual on Uniform Traffic Control Devices. They also experienced a degraded lane line condition, where longitudinal marks were present but were shorter sideways C-shaped lines and irregularly spaced (Figure 3) 600 feet from the pedestrian. All trials for this test were conducted in a high sun angle condition (sun altitude > 40 degrees).



Figure 2: Pedestrian test environment. Defined lanes are marked in white and the degraded lanes condition are marked in yellow.

For each trial, the vehicle started in a defined lane and accelerated to a speed of 40 mph, with both adaptive cruise control and automatic steering activated at this point. Traffic cones were positioned on either edge of the roadway 350 feet prior to the pedestrian rig, and the pedestrian began crossing the road as soon as the vehicle passed these cones at a speed of 5 fps (Figure 2). This was designed to result in a “near miss” scenario, where the vehicle would come within approximately 2 seconds of colliding with the pedestrian, but the pedestrian would be just out of the vehicle’s path even if the vehicle did not brake. The ADAS was reset between each trial at the locations marked start.

The pedestrian target consisted of a black Seasons™ rubber composite inflatable pedestrian (Figure 2: **Pedestrian test environment**). The pedestrian was 72 inches tall and dressed in a plain long-sleeve shirt and blue jeans. It was continuously reinflated throughout testing to minimize changes in appearance due to air loss. The rig moving the pedestrian was supported by two 8-foot wooden posts placed on either side of the roadway and secured using 114 pounds of concrete. A 75-foot Keeper™ 3/8-inch bungee cord was suspended between the two posts, also secured to the ground on either side. The cord tension provided just enough sag so that the pedestrian would touch the ground while suspended from the cord without hovering or bending. A nylon rope connected to the top pedestrian’s head was pulled by an operator on the side of the track. The operator manually pulled the pedestrian during each trial, using a digital clock to pace the movement so that the pedestrian would travel at the intended speed.

Each of the six vehicles completed 20 randomized and counterbalanced trials in the defined lane condition and 20 trials in the degraded lane condition.

Table 4 summarizes the design matrix for this experiment.

Table 4: Pedestrian test design matrix

Model	Number of Vehicles	Trials per vehicle	Lane marking quality
A	3	20	Defined
	3	20	Degraded
B	3	20	Defined
	3	20	Degraded



Figure 3: Degraded lane marking appearance

Data Collection Instruments



Figure 4: Pedestrian test environment layout

Several forms of data were conducted during each trial. First, in all experiments continuous video data was captured from cameras covering three areas of interest: (1) the driver's face and hands, (2) the road, and (3) the console readout displaying ADAS information. These cameras were GoPro Hero 7 Black models. The road-facing camera was mounted in the center of the dashboard set back 3 inches from the front of the windshield. The driver-facing camera was mounted at a position specific to each model and standardized using dashboard landmarks. The position of the console-facing camera varied depending on where information was displayed in each vehicle model.

For vehicles with ADAS information presented on the center console (Model B), this camera was mounted on the sun roof just behind the first row of seats using a suction mount. For vehicles with ADAS information presented behind the steering wheel (Model A), this camera was mounted on the steering column. This required removing the GoPro arm attachment from the standard cage and replacing it with flat adhesive strips. It was then placed along the center line of the steering column as far forward as possible, with the bottom of the camera's sensor resting on the bottom lip of the console alcove. This placement allowed the camera to capture a full view of the console without blocking the driver's view of the console.

Cameras were set to prohibit auto-exposure adjustment so that light capture was as similar as possible across trials. The video capture was set to 25 fps with a 1,920 by 1,440 pixel image size. Zoom was set to the highest level of lens resolution available. Each camera was electronically connected to a SyncBac Pro radio frequency synchronizer device, which augments each collected video frame with a synchronized timecode. As a result, frames from each of the cameras could be related to each other by the time at which each frame was captured.

In addition to the camera data, a second set of instruments captured data on external ambient light as well as motion properties of each vehicle, including rotation and acceleration on each principal axis (Figure 5). These instruments consisted of two components electronically linked and synchronized to a single data acquisition device. The first component consisted of an Adafruit LIS3MDL magnetic orientation sensor and an Adafruit LSM6DSOX 3-axis accelerometer, which was attached to the steering wheel shaft. The magnetic orientation sensor measured the degree of steering deflection applied when the driver touched the steering wheel, as well as the magnetic compass heading of the vehicle.

The second component consisted of an Adafruit VEML7700 ambient light sensor mounted on the outside of the passenger-side window (Figure 5). The ambient light sensor collected data on raw luminosity as well as white light saturation. The light sensor measures ambient light and was calibrated to detect changes in high light intensity corresponding to direct sunlight. Each sensor communicated over a wired connection with an Adafruit Metro microcontroller (a variant of the Arduino Uno) placed within the vehicle and synchronized using the I2C communication protocol. The sensor array was synchronized with the cameras by using a sound cue that was presented when the sensors turned on and turned off, which was audible to each of the cameras.



Figure 5: Sensor components. Left: ambient light sensors. Right: acceleration and rotation sensor

Results

For all statistical tests, alpha = .05 unless otherwise noted. Appendix A contains pictures of all in-car alerts, as well as audio sounds. Appendix B includes all basic statistics for the highway test and Appendix C includes the descriptive statistics for the pedestrian test.

Highway Test

The goal of this test was to determine if sun angle (high and low) affected the types and rate of driver alerting during semiautomated hands-free driving. Six types of behaviors were observed at various points along the route, as listed in Table 5. The vast majority of the total 893 events were standard visual hands-on-wheel (HOW) alerts for both model cars, to which the driver always responded. Figure 6 illustrates these standard HOW events, including which sun angle and whether the car was headed into or away from the sun. Only Model B presented a few escalated urgent HOW visual alerts and aural alerts in Table 5 and only Model A suspended Autosteer during the trial. Also, only Model A experienced no events in a few trials.

The disparity in overall alerting counts between Models A and B is explained by different alerting intervals. Figure 7 shows the intervals between each adjacent pair of hands-on-wheel alerts, categorized by each car model and the sun angle category. There were 613 events including 130 events for Model A and 483 events for Model B vehicles. Model A vehicles experienced more variation in HOW intervals, with a minimum interval of 16 seconds and a maximum interval of 130 seconds (Appendix B, Table 12).

Table 5: Types of events that occurred during the highway test. Appendix A includes illustrations of alerts.

Event	Model A high	Model A low	Model B high	Model B low	Totals
Standard hands-on-wheel icon	122	136	292	317	867
Urgent hands-on-wheel icon	0	0	3	4	7
Standard alert sound (double chime)	0	0	3	4	7
Autosteer suspended	2	0	0	0	2
Autosteer resumed	2	0	0	0	2
Trials with no events	6	2	0	0	8

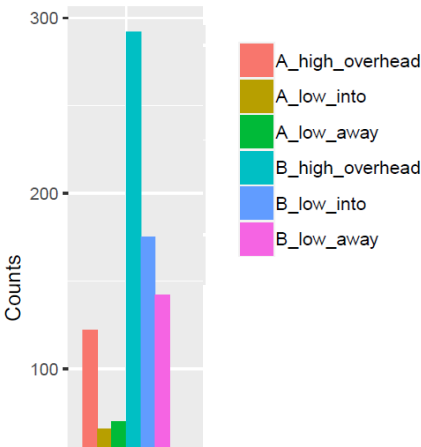


Figure 6: Counts of events separated by car and sun angle

Model B intervals were tightly grouped around 34 seconds (SD = 2 seconds). Unlike Model B, Model A vehicles had much more spread in the intervals between alerts, with an average interval of 52 seconds (SD = 24 seconds). Compared to Model A, Model B intervals were much shorter. This is why Model B vehicles produced more alerts than Model A, as seen in Figure 8 and Table 6. Interestingly, Model A intervals appeared to be in three distinct interval bands around 35 seconds, 75 seconds, and 110 seconds. We could not determine any factors that might explain these bands.

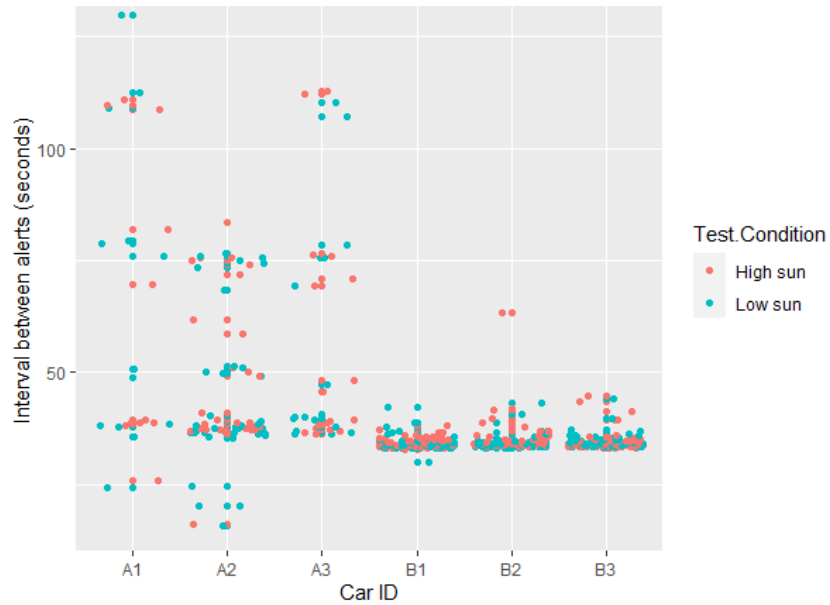


Figure 7: Hands-on-wheel intervals by individual car and sun angle

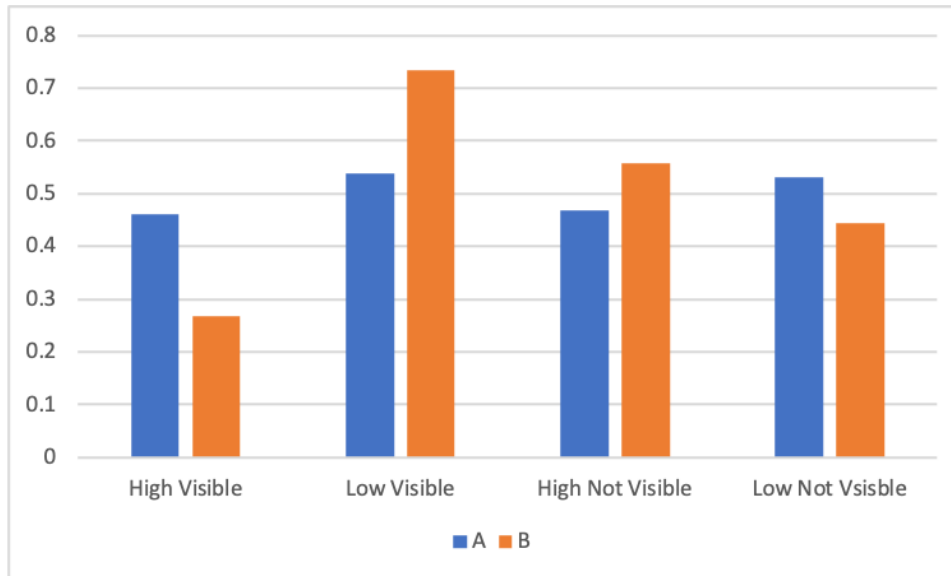


Figure 8: Percentage of Hands-on-Wheel alerts in the low and high sun angle groups where the sun was and was not visible

One experimental confound was the location of the sun in the sky and whether the camera in the car was in the line of sight to the sun. While generally an east/west route, the roads in Figure 1 curved slightly and tree tops would occasionally obscure the sun, as would passing cars. Even in the high sun position, occasionally the sun was visible. Thus, in order to accurately determine the influence of the sun, we reviewed every video and made a subset of those trials where a hand-on-wheel icon was displayed with the sun actually visible in the line of sight to the camera.

Table 6: Counts of Hands-on-Wheel events when sun was visible in the forward field

Car	Low sun	High sun	Total
Model A	28	24	52
Model B	121	44	165
Total	149	68	217

While roughly half of the 893 events were designed to be directly into the sun, only 24% (N=217) could be counted in any sun angle analysis. The overall counts are listed in Table 6. These results suggest that Model B exhibited different performance in different lighting conditions when the sun was in the forward field. On average, Model B alerted the driver 3 times more often than Model A overall, and almost 5 times more when the sun was low.

Figure 8 illustrates the percentages of HOW events when the sun was and was not visible for the two different car brands, categorized by the experimental sun angle condition. A chi square test looking at whether the number of alerts for Model A under low and high sun angles is independent from the visible versus not visible sun variable, the chi-square statistic = 0.007, $p = .93$ so there were no dependencies. For Model B, the chi-square statistic = 40.7, $p < .00001$, meaning the Model B HOW alerts were influenced by both sun angle and whether the sun was visible. Thus, Model A cars were generally consistent in their alerting, and Model B was more variable. Given the increased alerting frequency of Model B, to better compare the variability in HOW alerting for Model A and B vehicles, Figure 9 shows the z scores for each of the vehicle's HOW occurrences, which normalizes each car by its unique class mean and standard deviation. It also distinguishes between events where the sun was and was not visible.

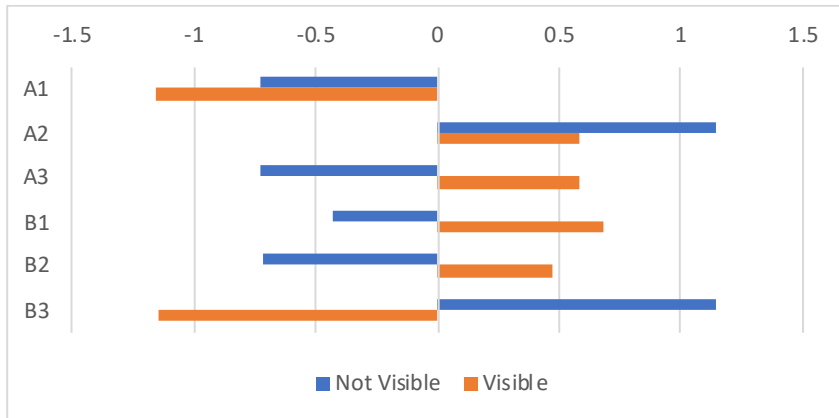


Figure 9: Normalized z scores for individual vehicles by their model average

Cars A1 and A2 were consistent across both sun settings. Model A vehicles as a group were slightly less variable than Model B cars with the sun visible, while Model B cars were less variable when the sun was not visible. It should be noted that overall variability across both model groups was lower in the cases where the sun was not visible, suggesting that sun glare could have an important effect on HOW alerting.

To further determine any effect of sun glare, we examined every HOW event with the sun visible in the forward field to determine if there were any differences in the horizontal and vertical positions of the sun when an alert was generated. Using the lower left of the windshield as the 0,0 position and normalizing between cars, we plotted the pixel position of the sun for every HOW event per car with a visible sun. The results are shown in Figure 10, while Figure 11 shows the averages.

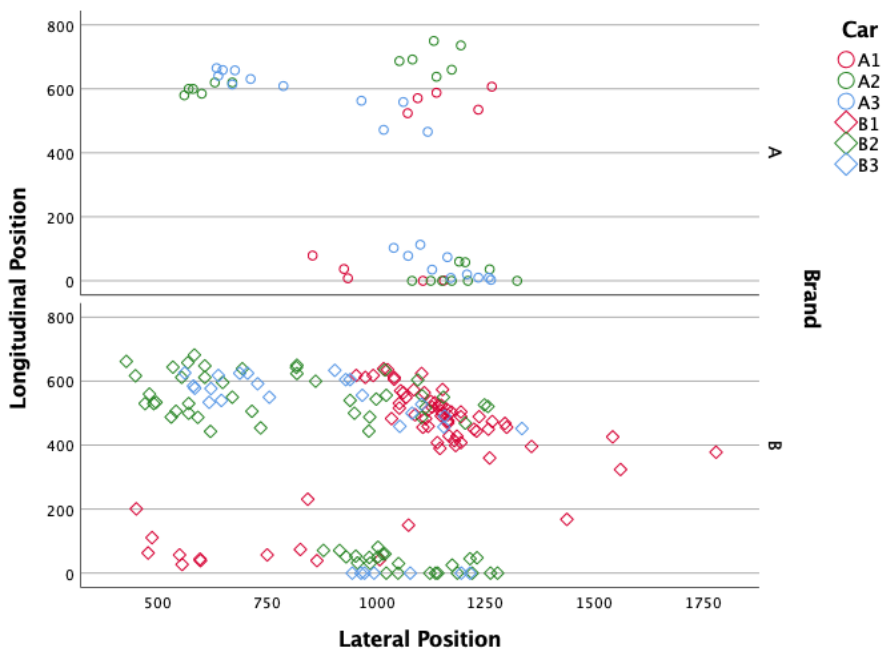


Figure 10: Lateral and longitudinal position of the visible sun when a hands-on-wheel alert sounded

A multivariate analysis of variance (MANOVA) was conducted with the six different cars as the first independent variable, with low versus high sun angle as the second. The pixel horizontal and vertical locations of the sun were the dependent variable. Results showed that the vertical and horizontal positions of the sun were no different between all six cars ($F(5,205) = 2.027, p = .076$ and $F(5,205) = 2.151, p = .061$, respectively). However, sun angle and the interaction between sun angle and car were both significant for the lateral and longitudinal positions (sun angle lateral: $F(1,205) = 7.4, p = .007$, sun angle longitudinal: $F(1,205) = 2169.2, p < .001$, interaction lateral: $F(5,205) = 27.6, p < .001$, interaction longitudinal: $F(5,205) = 10.4, p < .001$).

The significance for the overall sun angle from low to high was expected, as this was core to the experimental design. Figure 10 illustrates that all cars experienced alerting in the lateral direction in a similar pattern; however, Car B1 suffered the widest difference at almost 500 pixels difference to the right, also confirmed in Figure 11. This is important because Car B1 had a slightly higher location for alerting under high sun angle conditions, but also lower than all other cars in the low sun angle position, and is the primary driver behind the significant statistics in the MANOVA.

The MANOVA results indicate that regardless of the model, cars typically alerted the driver for a HOW event with the sun in the same general vertical place in the sky. This was also true on average for the lateral location of the alerts, indicating that in general, both car models did not significantly differ in where alerts were triggered, with the exception of one Model B car, which was very different from all other cars.

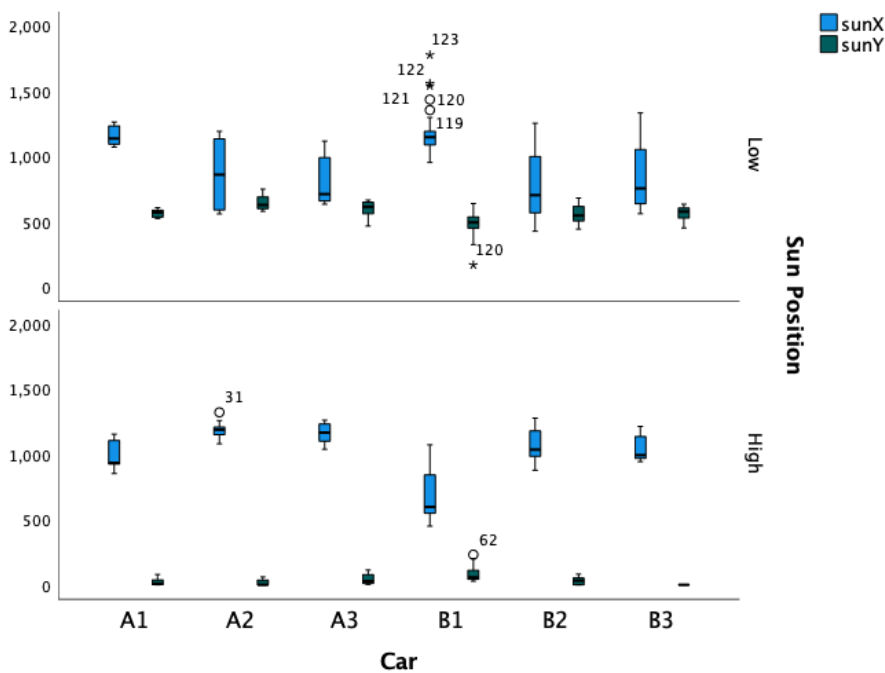


Figure 11: Sun position by individual car and sun X/Y for HOW events with a visible sun

When taken together, the results of the highway test indicate that there were no significant differences between models in where the sun was in the line of sight to the camera when a HOW alert sounded, save for one Model B outlier car. Model A produced HOW alerts consistently across all lighting conditions. However, Model B alerted its driver 3 times more often than Model A overall to a HOW event, and almost 5 times more when the sun was low. Indeed, these results showed that Model B HOW alerts were influenced by both sun angle and whether the sun was visible.

The intervals for Model A alerts were far more variable than Model B. Model A intervals could range from 16 seconds to more than 2 minutes, while Model B intervals were tightly clustered around a half minute. Another noteworthy result was what did not happen. Given the 613 HOW events for both cars, only Model B had an aural alert in addition to an escalated urgent visual alert. However, this only appeared in 7 instances. Moreover, there were 8 trials where the driver of Model A was allowed to drive for approximately 4.5 minutes with no hands on the wheel.

Pedestrian Avoidance Test

The goal of this test was to investigate a possible interaction between lane and pedestrian detection, especially in the presence of degraded lane lines, as well as assessing driver alerting in these scenarios. For the 120 trials for Model A in both the defined and degraded line conditions, none resulted in pedestrian detection, alerting, or any braking maneuvers.

Model B experienced 123 trials due to concerns about possible lost data and during these trials, nine behaviors were observed as the vehicle approached the pedestrian (Table 7). The car detected the pedestrian in 99% of cases but only braked for 85% of these events. Indeed, in 3 cases (2.4% of all trials), the cars automatically accelerated into the pedestrian, which will be discussed in more detail in a later section. Some, but not all, of these occurred in concert, i.e., a hands-on-wheel alert and aural alert could sound in quick succession, but there was no predictable pattern of the combination of visual and/or aural alerting in either lane line condition.

Table 7: Event types for Model B only. Appendix A includes illustrations of alerts.

Event name	Count
Standard hands-on-wheel icon	25
Urgent hands-on-wheel icon	3
Standard alert sound (double chime)	25
Urgent alert sound (rapid alarm)	20
Forward collision warning icon	8
Takeover alert icon	1
Pedestrian visualization icon	122
Automatic braking	103
Automatic acceleration	3

Error! Reference source not found. shows the counts of events in Table 7 for defined and degraded lanes per car for all events except pedestrian visualizations, which will be analyzed further in a later section. Automatic braking was very consistent for cars B1 and B2, but Car B3 only braked in about 60% of all trials. It is especially noteworthy that Model B cars only provided standard HOW visual and aural alerts in the degraded lines conditions, with Car B2 providing 3 times the standard visual and aural alerts of Car B1. These alerts seemed to be commensurate with the automatic braking events, but only for Car B2.

There were no standard alerts for Car B3, but it had the highest number of urgent aural alerts and the only visual HOW urgent alert. And other than a single alert for Car B2, Car B3 was the only car that sounded the forward collision warning, and these occurred in both lane conditions. Only Model B cars in the defined lines category experienced automated acceleration events in the presence of a pedestrian, and all three cars did this 1 time each.

It is important to remember that in the majority of trials, no alerting was provided other than just the visual pedestrian icon (63%, Car B1 = 32, Car B2 = 19, Car B3 = 26), and aural alerting was only present in

37% of trials. In these cases, if a driver was not paying attention to the display or the road, the risk would have been extremely high for possible contact.

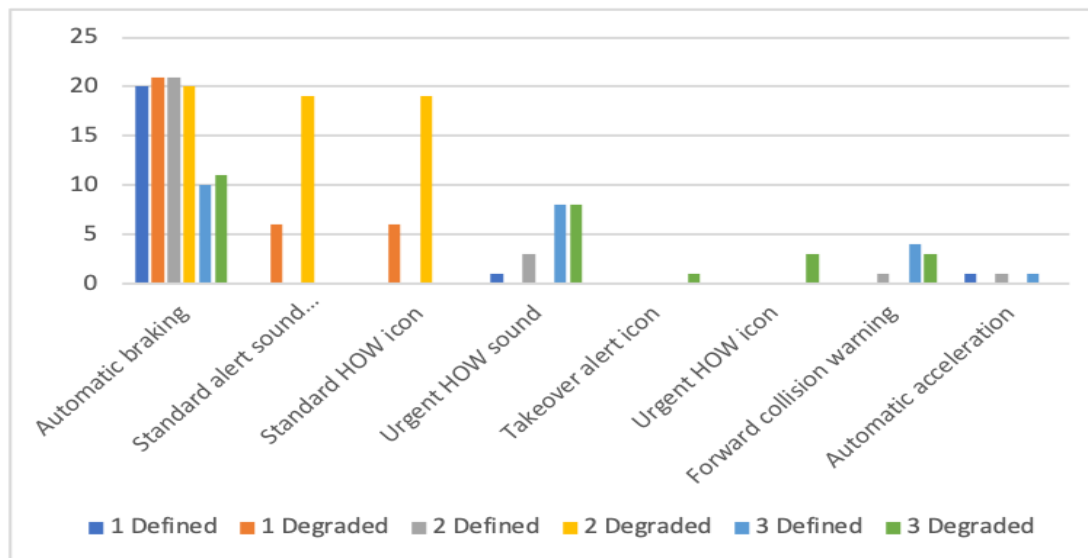


Figure 12: Counts of Model B events by individual car and lane condition

Table 8 provides summary statistics for where each car visualized the pedestrian in each lane marking condition. Cars B1 and B2 were largely consistent in where they initiated alerting, detecting the pedestrian slightly earlier (larger longitudinal values and negative lateral values). Car B3 detected the pedestrian much later, first detecting the pedestrian when the vehicle was 100 feet further down the road and the pedestrian was 10-20 feet further along its path. Appendix C provides the diagonal distances to the pedestrian and angle off each vehicle’s nose.

Table 8: Mean lateral and longitudinal distances to pedestrian visualizations in feet. Negative numbers mean the pedestrian was detected to the left of the vehicle centerline.

Cars	Lane Quality	Long. Mean (Std. Dev.)	Lat. Mean (Std. Dev.)	N
B1	Degraded	223.6 (37.7)	-10.3 (9.0)	21
	Defined	193 (55.3)	-2.7 (6.1)	20
B2	Degraded	204.3 (10.0)	-10.5 (4.8)	20
	Defined	201.4 (72.2)	-1.0 (5.7)	21
B3	Degraded	133.5 (47.0)	11.2 (2.4)	18
	Defined	104.4 (59.9)	6.7 (5.0)	22

Figure 13 shows the position of the inflated pedestrian, relative to the vehicle, when the pedestrian icon appeared on each car’s display. Longitudinal distance is the distance in feet from the car’s bumper to the pedestrian. Lateral distance is defined relative to the vehicle centerline (which was centered on the roadway), with -20’ at the far-left edge of the road and +20’ at the far-right edge of the road. Since the pedestrian detection crossed the road from left to right, an early detection of the pedestrian occurs with larger longitudinal distances and negative lateral distances (closest to the left edge, where the pedestrian began its movement). Small longitudinal distances and positive lateral distances indicate that the pedestrian was detected later.



Figure 13: Relative position of pedestrian target to vehicle when pedestrian icon appeared in Model B console

When comparing the estimated marginal means for the data in Table 8 through pairwise testing using a Bonferroni adjustment, for both the lateral and longitudinal cases, cars B1 and B2 are statistically no different, but Car B3 is ($p < .001$ for all comparisons with an alpha = .017 for a familywise error correction). The longitudinal comparison between defined and degraded lanes was not statistically significant at $p = .026$ but it was for the lateral data ($p < .001$). All this means that there was not likely a measurable difference in where the pedestrians were detected longitudinally by the different cars, but there was laterally with Car B3 performing very differently than Cars B1 and B2. It should also be noted that cars B1 and B2 both detected the pedestrian *earlier* in the degraded line conditions, by on average 7 and 9 feet respectively. However, Car B3 detected the pedestrian in the degraded lane lanes, on average, 4.5 feet after the defined line conditions. However, the most dangerous, i.e., late, detections happened primarily for Car B3 in the defined lanes condition.

Automatic Acceleration Events

As noted previously, there were 3 events where a car automatically accelerated in the presence of a pedestrian. All of the events occurred in the defined lane quality experimental condition, and each car experience 1 such event. These events are visualized in Figure 14. For Car B3, the pedestrian was visualized at 219 feet away, the car executed an automated braking maneuver 171 feet from the pedestrian, but then accelerated at 92 feet from the pedestrian. Then the driver was presented with an alarm and a forward collision warning. None of the 3 events were similar in the ordering or even the nature of the events in the timeline. The only similarity across all 3 events was that they occurred in the defined lanes conditions. This finding is unexpected since driving with lane lines represents the ideal operational domain that the car is expected to handle. The vehicle did not collide with the pedestrian target in any test.

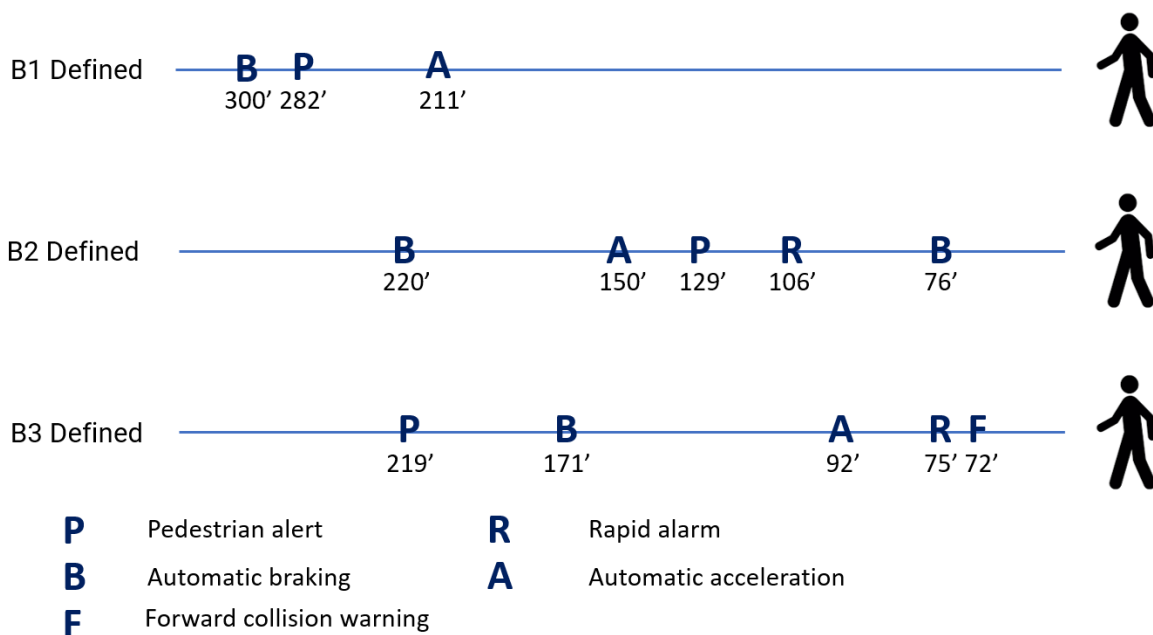


Figure 14: Distances between car and pedestrians when automated acceleration events happened

Discussion

The Highway Test

The goal of the highway test was to determine if low and high sun angles affected the types and rate of driver alerting during semiautomated hands-free driving, when the sun was in a direct line of sight to the camera. For one of the two models tested, there appeared to be no statistical relationship between if the sun was in the forward field at either a low or high sun angle. There was, however, a clear statistical relationship that suggested Model B Hands-on-Wheel alerts are influenced by both sun angle and whether the sun was visible.

Model B cars alerted the driver to a HOW event more often in the low sun angle condition, between 4 and 20 degrees elevation, than when the sun exceeded 40 degrees elevation. This suggests some kind of dynamic adaptation where the onboard autonomy is aware of the higher risk condition and increases alerts accordingly. Such adaptations are critical in helping drivers not become complacent when the environmental conditions, like sun glare, can make it harder for drivers to see and react to emerging threats. However, these results also demonstrated wide variation between cars and even within a single car. Model A vehicles had widely varying alert intervals and Model B cars were more variable in both the number of alerts per vehicle but also where the alerts occurred for one car. These results raise the issue that possibly one or more cameras were not correctly calibrated, and future work is needed to determine whether this could be an underlying safety issue.

Lastly, these results raise important questions about how long is too long for drivers to have their hands off the steering wheel. Model B alerted drivers more often overall and consistently would not let drivers go more than about half a minute without their hands on the wheel. In contrast, Model A would sometimes keep the interval short (16 seconds) but on average would not alert drivers to the need to be hands on. Indeed, there were 8 trials where drivers of Model A cars were allowed to drive for approximately 4.5 minutes with no hands on the wheel.

Driver distraction is a serious problem that directly contributes to the increasing deaths on U.S. roadways and such permissive policies only encourage bad driving behavior. Moreover, both models predominantly relied on visual warnings to alert drivers to the need to put their hands on the wheel, which may not be seen if a driver is indeed distracted. Such events should also include an aural warning to ensure drivers are aware that their attention may be critically absent.

The Pedestrian Test

The pedestrian tests revealed wide discrepancies across different kinds of cars with onboard autonomy, and also significant variation across individual vehicles of the same type. First, Model A never detected the pedestrian out of 120 trials and thus never executed any minimum risk behaviors. The conditions were ideal, with a bright sunny sky with a dark pedestrian crossing at an expected pace. The lack of any detection or risk mitigation suggests that if the driver was even slightly inattentive, the outcome could have been disastrous.

The other group of cars from Model B performed much better, detecting the pedestrian in almost all scenarios. However, despite the presentation of 123 nearly identical scenarios, the three different cars in the Model B cluster did not exhibit consistent performance. Cars B1 and B2 were more consistent on where they first identified the crossing pedestrian as well as executing automatic braking. However, these two cars were not consistent with each other or with themselves in when or where they provided the driver with aural and visual alerting.

Car B3 was a statistical anomaly in terms of where it detected the pedestrian, providing much less advanced warning than the other two vehicles. It detected the pedestrian with 100 fewer feet of stopping distance, and after the pedestrian had already crossed the path of the vehicle, as opposed to the cars B1 and B2, which usually detected the pedestrian before it crossed the centerline. Car B3 did provide a few additional alerts other than the pedestrian visualization, but given its significant reduction in automatic braking (only 50% of its overall trials) and general lack of alerting, it was distinctly more unsafe than the other two Model B cars.

One of the stated goals of this research was to determine whether the degraded lane lines had a measurable effect on performance, and it did not appear to affect automatic braking for any of the cars. However, Cars B1 and B2 both consistently had the earliest pedestrian lateral detections in the degraded lanes condition, suggesting that the cars' attempts to find the lane lines may have helped them detect the pedestrian slightly earlier than in the defined lanes condition. Neither Car B1 or Car B2 provided any HOW alerts in the defined lane condition, suggesting these cars initiated these warnings strictly due to the loss of lane lines. In comparison, Car B3 issued higher level alerts in both defined and degraded lane conditions, as well as forward warning collision alerts, so it is not clear if the presence of a pedestrian and the lack of lane lines could have influenced the generation of these alerts.

Lastly it should be noted that while a low percentage, each of the cars inappropriately accelerated in the presence of a pedestrian. In two cases, the car accelerated *after* the car clearly detected the pedestrian, and in the third case, accelerated after an automatic braking maneuver but before the pedestrian icon was displayed. That such behavior was seen in such a limited test environment and in the best possible testing conditions (defined lane lines, sunny day, dedicated test track) should be cause for alarm.

These results raise an important issue surrounding the predictability of an autonomous system. While Model A never detected the pedestrian and Model B almost always detected the pedestrian, it should not automatically be assumed that one system is better than the other. Indeed, Model B accelerated towards the pedestrian in three cases, and none of the three Model B cars were consistent with each other or even internally. This is especially problematic because drivers in Model A likely never trust their cars to detect and avoid pedestrians and thus, are likely on high alert in pedestrian-rich environments. Model B drivers may be lulled into a false sense of security in these settings, assuming that cars are actually more capable than they are. These drivers are then likely surprised and unprepared to take over in the 2.4% of scenarios where an unexpected and dangerous autonomous action occurs, setting up the driver and all other nearby stakeholders for potentially deadly outcomes.

Conclusion

Two sets of tests were conducted to examine if and how sun glare affected driver alerting on the highway and also to determine if there was any interaction between pedestrian detection and the quality of lane lines. Results demonstrated that at least one ADAS-equipped model can adapt to low sun conditions to mitigate glare and this same model could reliably detect a pedestrian. However, in all tests and for all cars, there was large variation in individual car performance, with sometimes very surprising and unsafe behavioral outcomes.

This issue of surprising behaviors more broadly speaks to the critical problems with significant variation both between cars of different models but also within a single model or even a single vehicle. Both the highway and pedestrian tests illustrated that in current ADAS-equipped cars on U.S. roadways, there are a number of behaviors that can wildly vary, potentially catching drivers off guard (like surprise accelerations) or lull them into a false sense of security (being allowed to stay hands free for more than 2 minutes on the highway.) There is a long history of operators becoming complacent and performing worse with imperfect or unreliable automation than with no or obviously bad automation in the aviation domain (Parasuraman & Manzey, 2010; Rovira, McGarry, & Parasuraman, 2007; Wickens, Clegg, Vieane, &

Sebok, 2015), so it is critical that the autonomous surface transportation community incorporate these lessons as quickly as possible, and improve driver monitoring and alerting.

Lastly, both these tests highlight the urgent need for regulatory standards that set clear performance expectations so that ADAS-equipped cars do not present an unreasonable risk to the public. This is the area of current focus, as more research is needed to determine “good enough” performance standards for cars that embed probabilistic reasoning, with resulting performance that can widely vary for cars of the same make and model.

References

- AAA. (2022). AAA Testing Finds Inconsistencies with Driving Assistance Systems [Press release]
- Bauchwitz, B., & Cummings, M. L. (2022). Individual Differences Dominate Variation in ADAS Takeover Alert Behavior. *Transportation Research Record: Journal of the Transportation Research Board*, 2676(5), 489-499. doi:10.1177/03611981211068362
- Choi, H. C., Park, J. M., Choi, W. S., & Oh, S. Y. (2012). Vision-based fusion of robust lane tracking and forward vehicle detection in a real driving environment. *International Journal of Automotive Technology*, 13(4), 653–669.
- Cicchino, J. B. (2022). Effects of automatic emergency braking systems on pedestrian crash risk. *Accident Analysis & Prevention*. doi:10.1016/j.aap.2022.106686
- Combs, T. S., Sandt, L. S., Clamann, M. P., & McDonald, N. C. (2019). Automated Vehicles and Pedestrian Safety: Exploring the Promise and Limits of Pedestrian Detection. *American Journal of Preventive Medicine*, 56(1), 1-7.
- Cummings, M. L., & Bauchwitz, B. (2022). Safety Implications of Variability in Autonomous Driving Assist Performance. *IEEE Intelligent Transportation Systems*, 23(8), 12039-12049.
- Dunn, N., Dingus, T., & Soccolich, S. (2019). *Understanding the Impact of Technology: Do Advanced Driver Assistance and Semi-Automated Vehicle Systems Lead to Improper Driving Behavior?* Retrieved from Washington DC:
- Esfahani, M. A., & Wang, H. (2021). Robust Glare Detection: Review, Analysis, and Dataset Release. *arXiv:2110.06006*.
- Gross, A. (2022). Consumer Skepticism Toward Autonomous Driving Features Justified.
- Huang, Q., & Liu, J. (2021). Practical limitations of lane detection algorithm based on Hough transform in challenging scenarios. *International Journal of Advanced Robotic Systems*, 1-13. doi:10.1177/172988142110087
- Huang, Q., & Liu, J. (2021). Practical limitations of lane detection algorithm based on Hough transform in challenging scenarios. *International Journal of Advanced Robotic Systems*, 18(2).
- J.D. Power. (2022). *J.D. Power 2022 Mobility Confidence Index Study*. Retrieved from Troy, MI:
- Kim, J., Han, D. S., & Senouci, B. (2018). *Radar and Vision Sensor Fusion for Object Detection in Autonomous Vehicle Surroundings*. Paper presented at the IEEE Tenth International Conference on Ubiquitous and Future Networks (ICUFN), Prague.
- Kong, H., Audibert, J. Y., & Ponce, J. (2009). *Vanishing point detection for road detection*. Paper presented at the IEEE Conference on Computer Vision and Pattern Recognition, Miami, FL.
- Laris, M. (2018). Fatal Uber crash spurs debate about regulation of driverless vehicles. *Washington Post*.
- Liu, W., Li, S., & Huang, X. (2014). International Journal of Computer Mathematics. *Extraction of lane markings using orientation and vanishing point constraints in structured road scenes*, 91(11), 2359–2373.
- Loveday, S. (2019). How Does Tesla Autopilot Fare Driving Directly Into The Sun? Retrieved from <https://insideevs.com/news/343151/how-does-tesla-autopilot-fare-driving-directly-into-the-sun-video/>
- Macek, K. (2022). *Pedestrian Traffic Fatalities by State: 2021 Preliminary Data*. Retrieved from Washington DC:
- Matsushita, Y., & Miura, J. (2011). On-line road boundary modeling with multiple sensory features, flexible road model, and particle filter. *Robotics and Autonomous Systems*, 59(5), 274–284.
- Mueller, A. S., Cicchino, J. B., & Calvanelli, J. V. (2022). *Habits, attitudes, and expectations of regular users of partial driving automation systems*. Retrieved from Arlington, VA:

- NHTSA. (2022a). *Early Estimate of Motor Vehicle Traffic Fatalities in 2021*. (DOT HS 813 283). Washington DC: US Department of Transportation
- NHTSA. (2022b). *Summary Report: Standing General Order on Crash Reporting for Level 2 Advanced Driver Assistance Systems* (DOT HS 813 325). Retrieved from Washington, DC:
- Parasuraman, R., & Manzey, D. H. (2010). Complacency and bias in human use of automation: an attentional integration. *Human Factors*, 52(3), 381-410.
- Rajaram, R. N., Ohn-Bar, E., & Trivedi, M. M. (2015). *An Exploration of Why and When Pedestrian Detection Fails*. Paper presented at the IEEE 18th International Conference on Intelligent Transportation Systems, Grand Canaria, Spain.
- Rovira, E., McGarry, K., & Parasuraman, R. (2007). Effects of imperfect automation on decision making in a simulated command and control task. *Human Factors*, 49(1), 76-87.
- Tesla. (2021). Transitioning to Tesla Vision. Retrieved from <https://www.tesla.com/support/transitioning-tesla-vision>
- Wang, H., Wang, Y., Zhao, X., Wang, G., Huang, H., & Zhang, J. (2019). Lane Detection of Curving Road for Structural Highway With Straight-Curve Model on Vision. *IEEE Transactions on Vehicular Technology*, 68(6), 5321–5330.
- Waykole, S., Shiwakoti, N., & Stasinopoulos, P. (2021). Review on Lane Detection and Tracking Algorithms of Advanced Driver Assistance System. *Sustainability*, 13(20), 11417.
- Wei, J., He, J., Zhou, Y., Chen, K., Tang, Z., & Xiong, Z. (2020). Enhanced Object Detection With Deep Convolutional Neural Networks for Advanced Driving Assistance. *IEEE Transactions on Intelligent Transportation Systems*, 21(4), 1572–1583.
- Wickens, C., Clegg, B., Vieane, A., & Sebok, A. (2015). Complacency and Automation Bias in the Use of Imperfect Automation. *Human Factors*, 57. doi:10.1177/0018720815581940
- Yahiaoui, L., Uricar, M., Das, A., & Yogamani, S. (2020). *Let the Sunshine in: Sun Glare Detection on Automotive Surround-view Cameras*. . Paper presented at the Electronic Imaging, Autonomous Vehicles and Machines 2020.
- Yuan, J., Tang, S., Pan, X., & Zhang, H. (2014). *A robust vanishing point estimation method for lane detection*. Paper presented at the 33rd Chinese Control Conference Nanjing, China.
- Ziebinski, A., Cupek, R., Grzechca, D., & Chruszczyk, L. (2017). *Review of advanced driver assistance systems (ADAS)*. Paper presented at the International Conference of Computational Methods in Sciences and Engineering 2017 (ICCMSE-2017).

Appendix A: Car Event Pictures and Sounds

Table 9: Car console pictures of Model A when events happened

Event ID	Event Name	Picture
E1	Grey standard hands-on-wheel icon	 <p>The image shows the car's instrument cluster with a central digital display. The display shows a gear indicator 'D', a speed limit of 168 mph, and a recommended speed of 70 mph. A warning icon of a steering wheel with a hand on it is displayed, with the text 'Keep hands on steering wheel' below it. The speedometer on the right shows a reading of approximately 20 mph.</p>
E4	Autosteer suspended	 <p>The image shows the car's instrument cluster with a central digital display. The display shows a gear indicator 'D', a speed limit of 301 mph, and a recommended speed of 70 mph. A warning icon of a steering wheel with a hand on it is displayed, with the text 'Autosteer suspended' below it. The speedometer on the right shows a reading of approximately 20 mph. Below the main display, 'Drive Info' is shown: Trip 184.8 mi, Avg 36.7 mph, and Timer 03:35. The odometer at the bottom shows 89,627.8 miles.</p>




E5	Autosteer resumed	
----	-------------------	--

Table 10: Car console pictures of Model B when events happened

Event ID	Event Name	Picture
E1	Grey standard hands-on-wheel icon	
E2	Red urgent hands-on-wheel icon	

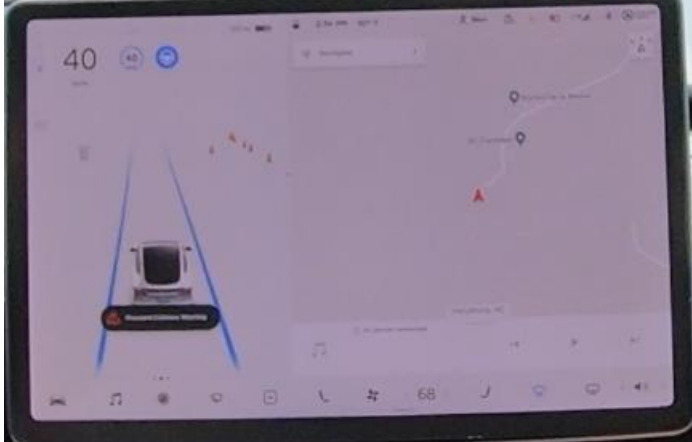
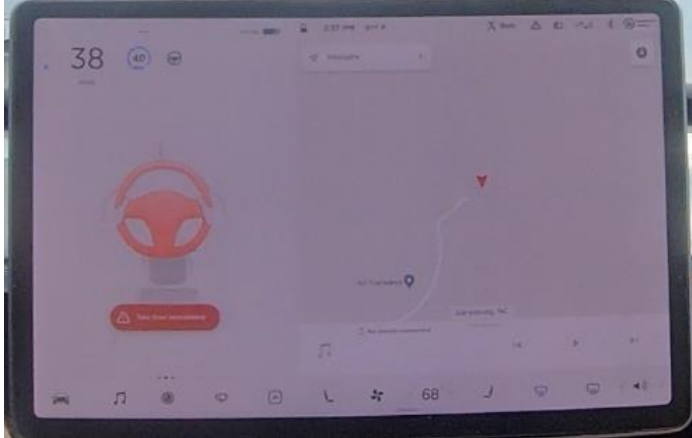
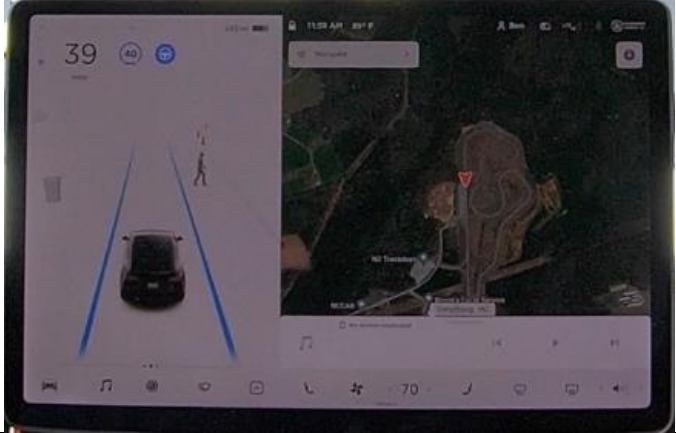


E7	Forward collision warning icon	
E8	Final takeover alert icon	
E9	Pedestrian visualization icon	

Table 11: Car event sounds of model B

Event ID	Event Name	Sound
E3	Standard alert sound (double chime)	 standard_double_chi me_sound.mp4
E6	Urgent alert sound (rapid alarm)	 rapid_alarm_sound.m p4

Appendix B: Highway Descriptive Statistics

Table 12: Descriptive statistics for hands-on-wheel alert intervals by car model in highway test

Car	Count	Mean [sec]	Min [sec]	Max [sec]	Median [sec]	SD [sec]
Model A	130	52.16	15.88	129.68	38.88	23.86
Model B	483	34.42	29.84	63.44	33.88	2.05

Table 13: Descriptive statistics for hands-on-wheel alert intervals by car model and sun angle in highway test

Condition	Count	Mean [sec]	Min [sec]	Max [sec]	Median [sec]	SD [sec]
A high sun	60	53.78	16.12	112.68	39.14	23.79
A low sun	70	50.77	15.88	129.68	38.40	24.01
B high sun	232	34.59	32.96	63.44	33.92	2.53
B low sun	251	34.27	29.84	44.20	33.88	1.48

Table 14: Descriptive statistics for hands-on-wheel alert intervals by car model and sun angle in highway test

Condition	Count	Mean [sec]	Min [sec]	Max [sec]	Median [sec]	SD [sec]
A1 high sun	11	63.64	25.80	110.84	39.52	33.56
A1 low sun	13	66.14	24.28	129.68	50.92	34.18
A2 high sun	31	48.35	16.12	83.44	38.80	17.13
A2 low sun	39	43.82	15.88	76.68	37.52	16.22
A3 high sun	18	57.10	36.32	112.68	42.62	25.60
A3 low sun	18	54.75	36.24	110.16	40.08	24.86
B1 high sun	78	34.26	32.96	38.20	33.90	1.05
B1 low sun	87	34.10	29.84	42.20	33.76	1.40
B2 high sun	75	35.02	33.40	63.44	34.00	3.74
B2 low sun	75	34.27	33.08	43.20	33.88	1.59
B3 high sun	79	34.51	33.20	44.84	33.84	2.07
B3 low sun	89	34.44	33.36	44.20	34.00	1.45

Table 15: Descriptive statistics for hands-on-wheel alert intervals by car and sun direction in low sun angle condition

Condition	Count	Mean [sec]	Min [sec]	Max [sec]	Median [sec]	SD [sec]
A1 Away	3	41.37	24.28	50.92	48.92	14.84
A1 Into	10	73.56	35.56	129.68	77.36	35.25
A2 Away	21	46.42	24.56	76.68	37.48	16.36
A2 Into	18	40.79	15.88	76.00	37.80	15.98
A3 Away	14	58.63	36.24	110.16	40.40	27.04
A3 Into	4	41.17	37.84	47.40	39.72	4.26
B1 Away	39	34.11	33.20	37.84	33.76	0.99
B1 Into	48	34.09	29.84	42.20	33.78	1.67
B2 Away	33	34.20	33.12	43.20	33.76	1.75
B2 Into	42	34.33	33.08	40.80	33.90	1.48
B3 Away	40	34.28	33.40	37.20	34.02	0.90
B3 Into	49	34.57	33.36	44.20	34.00	1.77

Table 16: Descriptive statistics for hands-on-wheel alert intervals by individual car and sun direction in high sun angle condition

Condition	Count	Mean [sec]	Min [sec]	Max [sec]	Median [sec]	SD [sec]
A1 Away	9	69.24	25.80	110.84	69.56	34.84
A1 Into	2	38.44	38.12	38.76	38.44	0.45
A2 Away	18	44.12	16.12	83.44	37.68	16.72
A2 Into	13	54.20	36.28	76.00	50.12	16.53
A3 Away	12	62.01	36.32	112.68	54.18	28.83
A3 Into	6	47.29	36.76	76.44	42.64	15.00
B1 Away	35	34.18	32.96	36.48	33.92	0.90
B1 Into	43	34.32	33.08	38.20	33.88	1.17
B2 Away	38	34.88	33.64	41.92	34.06	1.91
B2 Into	37	35.17	33.40	63.44	33.88	5.00
B3 Away	39	34.72	33.20	44.84	33.80	2.44
B3 Into	40	34.31	33.28	43.64	33.98	1.63

Table 17: Descriptive statistics for Sun X position by individual car when hands-on-wheel alert appeared with sun visible

Condition	Count	Mean	Min	Max	Median	SD
A1	10	1078.10	854.00	1265.00	1101.00	134.88
A2	21	1004.81	560.00	1323.00	1132.00	268.59
A3	21	979.38	634.00	1263.00	1062.00	230.70
B1	71	1082.93	450.00	1779.00	1128.00	240.11
B2	66	884.53	427.00	1278.00	955.00	257.46
B3	28	897.04	561.00	1334.00	942.50	228.15

Table 18: Descriptive statistics for Sun Y position by individual car when hands-on-wheel alert appeared with sun visible

Condition	Count	Mean	Min	Max	Median	SD
A1	10	295.00	0.00	607.00	301.50	286.45
A2	21	377.24	0.00	750.00	585.00	322.87
A3	21	332.95	3.00	665.00	466.00	286.76
B1	71	417.56	27.00	639.00	474.00	177.33
B2	66	366.65	0.00	682.00	500.00	261.24
B3	28	419.18	0.00	634.00	537.00	251.73

Appendix C: Pedestrian Descriptive Statistics

Table 19: Counts of pedestrian avoidance test trials

	Defined trials	Degraded trials	Total trials
B1	20	21	41
B2	21	20	41
B3	22	19	41

Table 20: Counts of alerts by individual car and lane quality of Model B

	No braking	Single alert	2 alerts	3 alerts	5 alerts	FCW	Driver takeover	Final takeover
B1 Defined	1	19	1	0	0	0	0	0
B1 Degraded	0	15	0	6	0	0	0	0
B2 Defined	1	18	2	1	0	1	0	0
B2 Degraded	0	1	0	19	0	0	0	0
B3 Defined	11	14	4	4	0	4	0	0
B3 Degraded	8	11	4	3	1	3	3	1

Table 20 shows counts of alerts depending on the individual car and lane quality for Model B. Single alert includes the pedestrian icon visualization. Two alerts typically include a pedestrian icon and a rapid alert. Three alerts include a pedestrian icon, a double chime, and a visual hands-on-wheel alert. Five alerts include a pedestrian icon, a rapid alert, a final takeover alert, a driver takeover alert, and a forward collision warning. FCW = forward collision warning.

Appendix C.1: Distances to Events

Table 21: Distance to pedestrian when the pedestrian icon appeared

Condition	Count	Mean [ft]	Min [ft]	Max [ft]	Median [ft]	SD [ft]
B1 Defined	20	193.0	51.4	282.4	211.0	55.3
B1 Degraded	21	223.6	166.4	300.2	229.8	35.6
B2 Defined	21	201.4	54.7	373.2	211.0	72.1
B2 Degraded	20	204.2	182.4	219.9	211.0	10.0
B3 Defined	23	104.4	13.0	219.9	116.2	58.9
B3 Degraded	18	133.5	47.5	219.9	128.9	46.9

Table 22: Distance to pedestrian when automatic braking occurred

Condition	Count	Mean [ft]	Min [ft]	Max [ft]	Median [ft]	SD [ft]
B1 Defined	20	181.7	65.4	300.2	202.9	58.2
B1 Degraded	21	203.2	166.4	266.8	202.9	27.5
B2 Defined	21	193.6	76.1	282.4	202.9	52.0
B2 Degraded	20	207.4	176.7	240.7	202.9	18.3
B3 Defined	12	140.7	85.3	176.7	158.4	37.5
B3 Degraded	11	142.7	61.6	202.9	157.5	44.8

Table 23: Distance to pedestrian when hands-on-wheel/double chime alert appeared

Condition	Count	Mean [ft]	Min [ft]	Max [ft]	Median [ft]	SD [ft]
B1 Defined	0	NA	NA	NA	NA	NA
B1 Degraded	7	138.2	123.9	161.8	133.9	14.7
B2 Defined	0	NA	NA	NA	NA	NA
B2 Degraded	20	145.0	63.5	195.5	166.4	36.2
B3 Defined	0	NA	NA	NA	NA	NA
B3 Degraded	0	NA	NA	NA	NA	NA

Table 24: Distance to pedestrian when rapid alert appeared

Condition	Count	Mean [ft]	Min [ft]	Max [ft]	Median [ft]	SD [ft]
B1 Defined	1	94.0	94.0	94.0	94.0	NA
B1 Degraded	0	NA	NA	NA	NA	NA
B2 Defined	3	84.4	58.6	106.0	88.5	24.0
B2 Degraded	0	NA	NA	NA	NA	NA
B3 Defined	8	68.7	16.0	80.6	75.3	21.5
B3 Degraded	8	85.5	53.2	123.9	81.5	23.4

Table 25: Distance to pedestrian when forward collision warning alert appeared

Condition	Count	Mean [ft]	Min [ft]	Max [ft]	Median [ft]	SD [ft]
B1 Defined	0	NA	NA	NA	NA	NA
B1 Degraded	0	NA	NA	NA	NA	NA
B2 Defined	1	86.9	86.9	86.9	86.9	NA
B2 Degraded	0	NA	NA	NA	NA	NA
B3 Defined	4	77.9	72.4	81.8	78.6	4.1
B3 Degraded	3	92.3	79.4	104.6	93.0	12.6

Table 26: Distance to pedestrian when driver takeover alert appeared

Condition	Count	Mean [ft]	Min [ft]	Max [ft]	Median [ft]	SD [ft]
B1 Defined	0	NA	NA	NA	NA	NA
B1 Degraded	0	NA	NA	NA	NA	NA
B2 Defined	0	NA	NA	NA	NA	NA
B2 Degraded	0	NA	NA	NA	NA	NA
B3 Defined	0	NA	NA	NA	NA	NA
B3 Degraded	3	83.9	65.4	107.5	78.8	17.6

Pedestrian alert

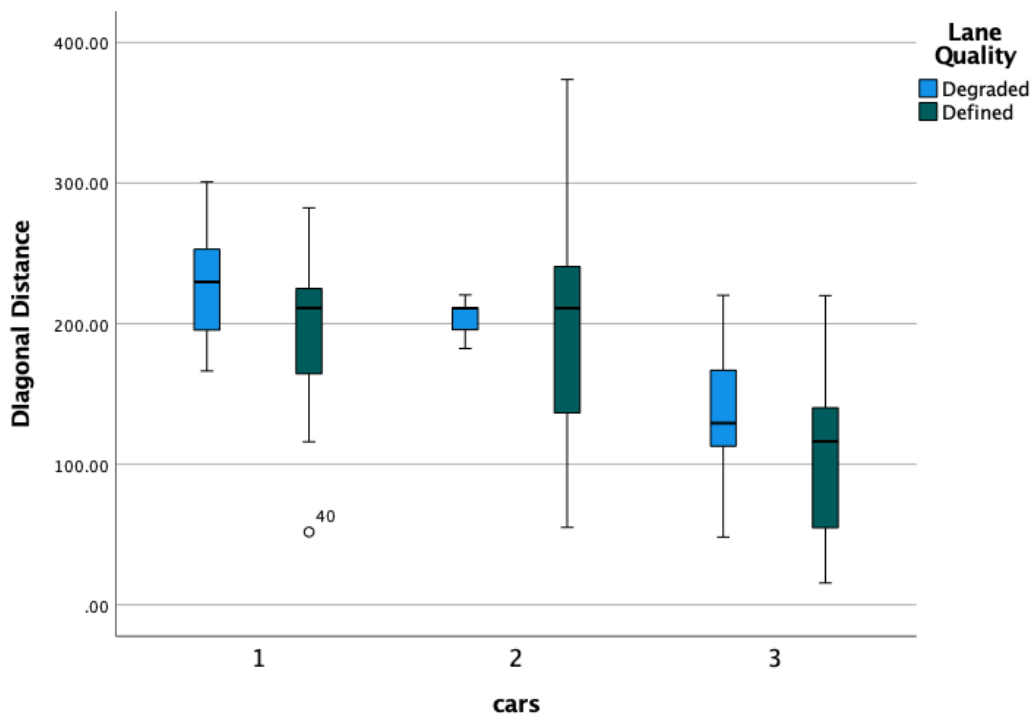


Figure 15: Diagonal distance when pedestrian alert appeared by individual cars of Car Model B

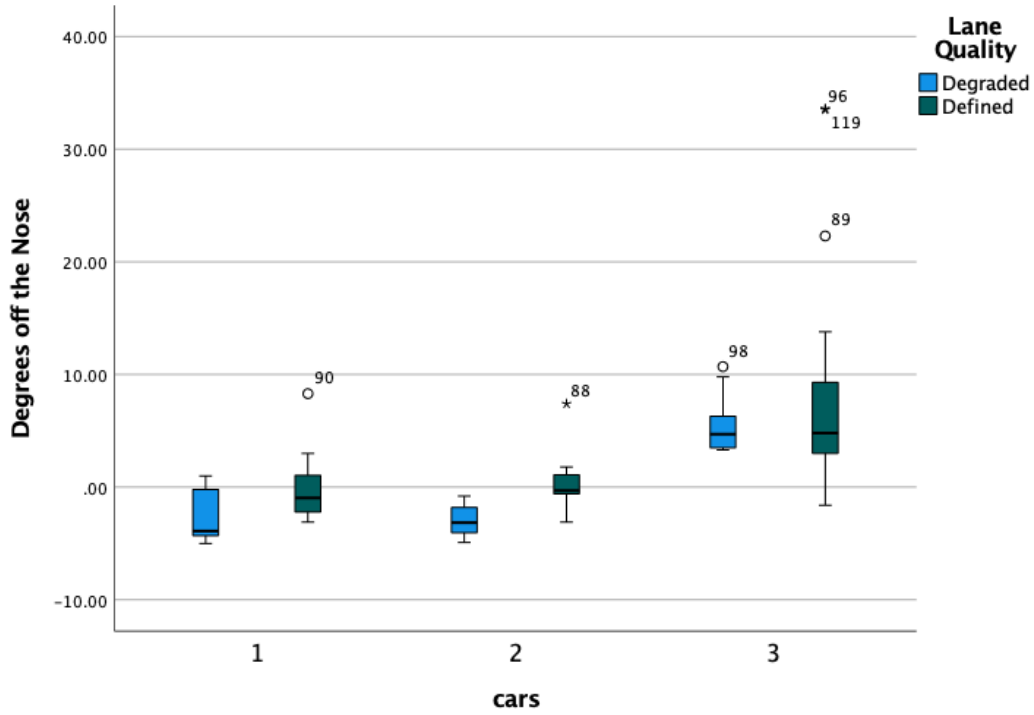


Figure 16: Degrees off the nose when pedestrian alert appeared by individual Model B cars

Automatic braking

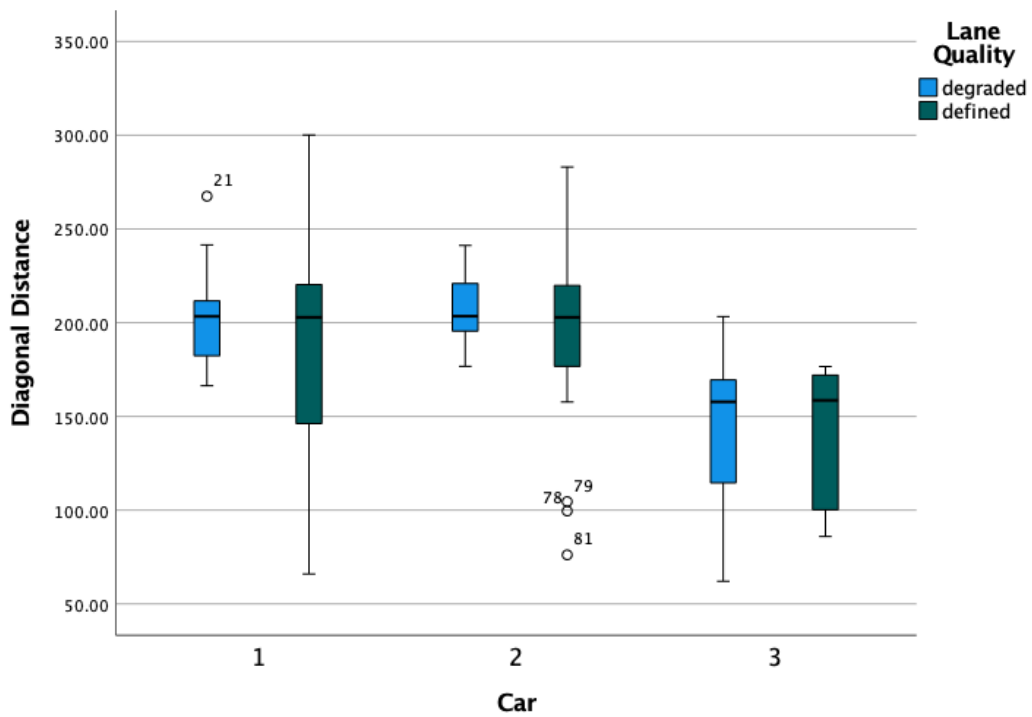


Figure 17: Diagonal distance when automatic braking occurred

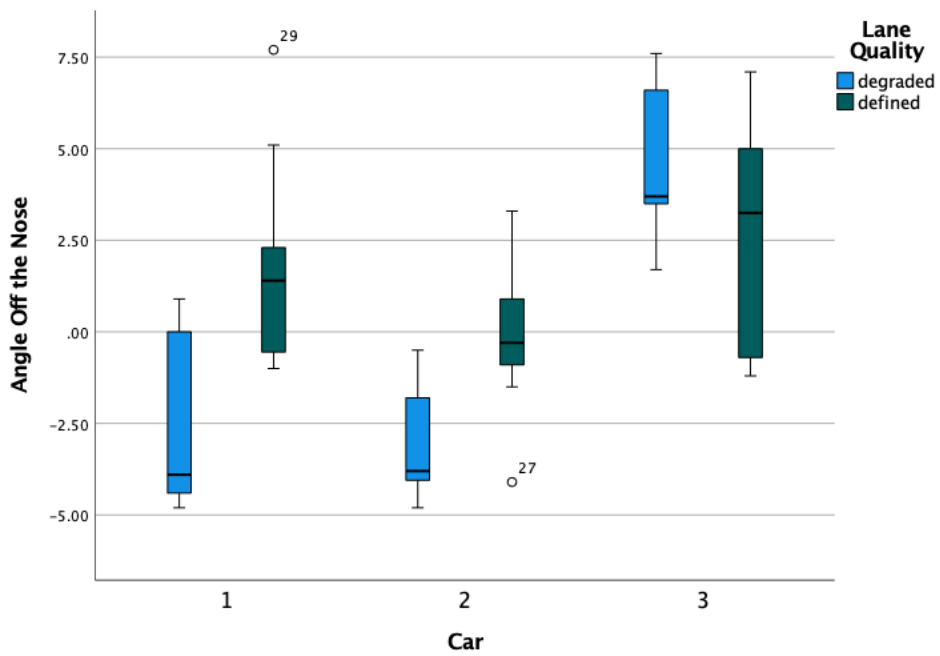


Figure 18: Degrees off the nose when automatic braking occurred

Hands on wheel/Double Chime

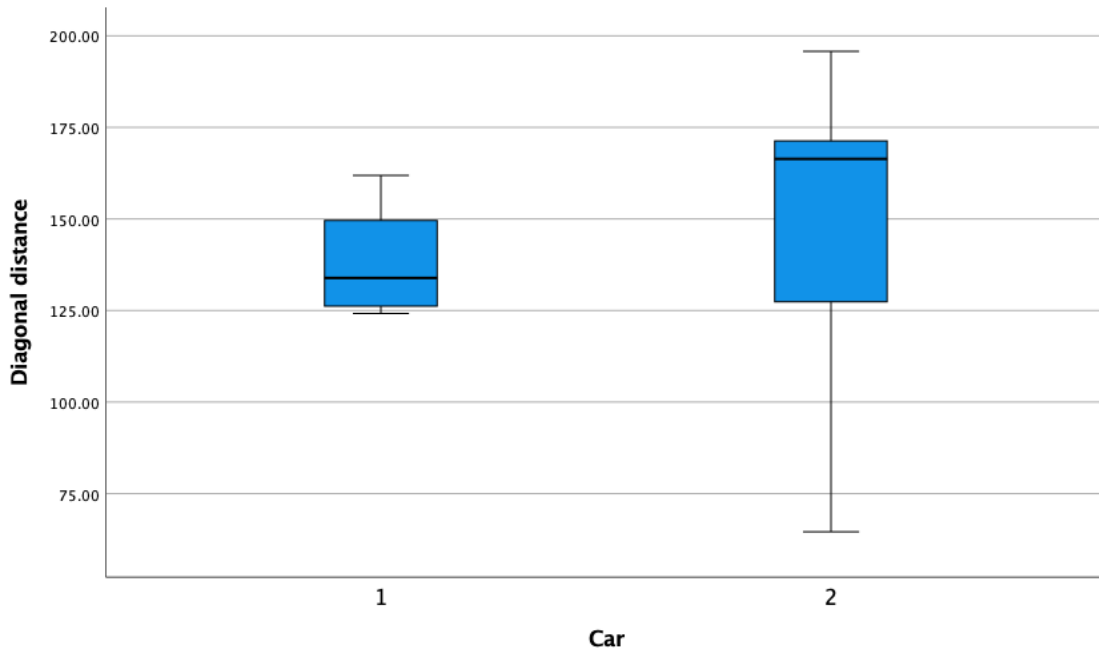


Figure 19: Diagonal distance of pedestrian when hands-on-wheel/double chime occurred

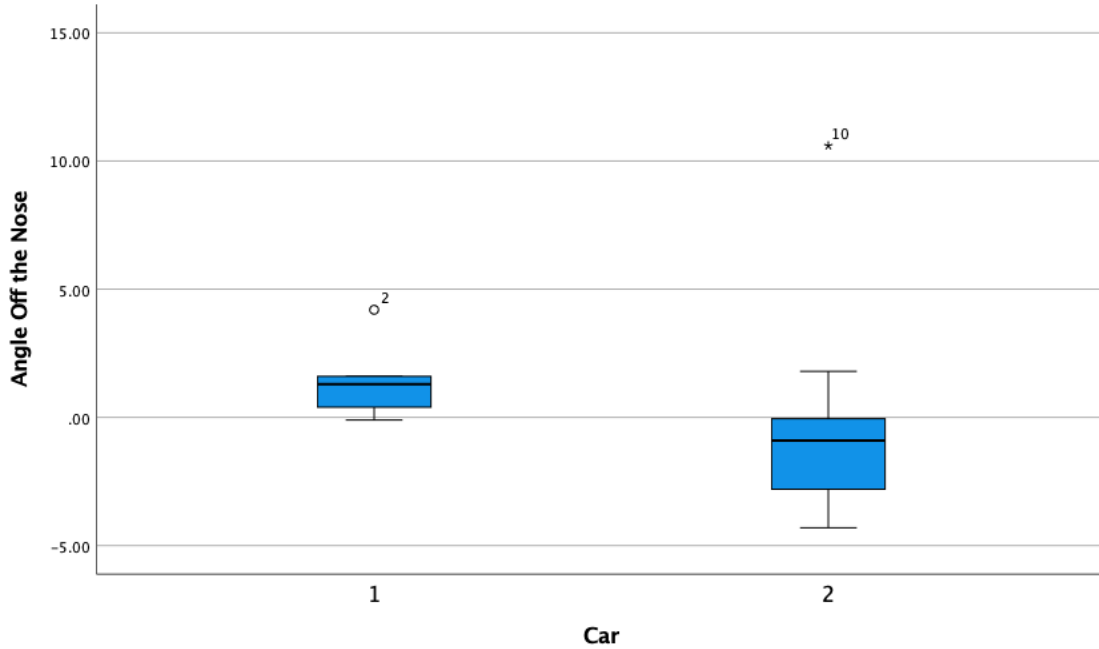


Figure 20: Degrees off the nose when hands-on-wheel/double chime occurred

Only B1 and B2 had hands-on-wheel or double chime alert with 6 cases of B1 and 19 cases of B2. Also, those happened only in degraded lanes.

Rapid alert

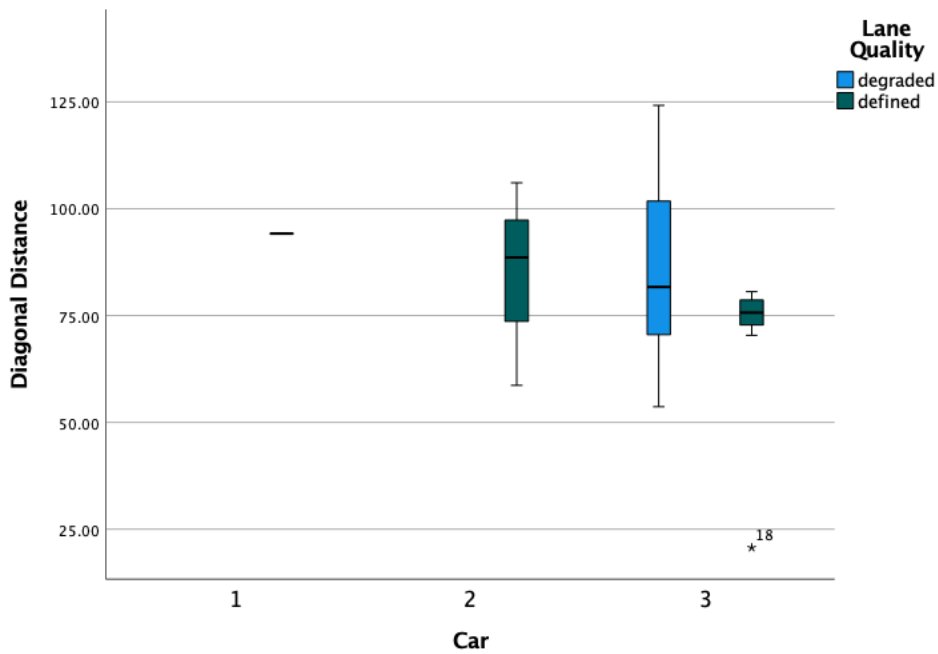


Figure 21: Diagonal distance when rapid alert appeared

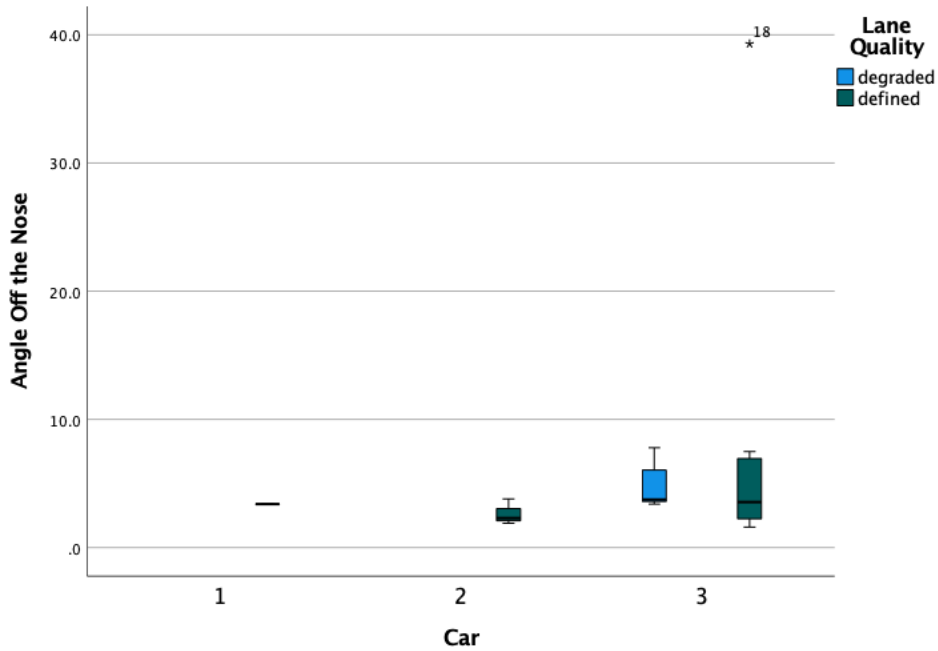


Figure 22: Angle off the nose when rapid alert appeared

Only Cars B2 and B3 experienced rapid alert cases, and they always happened to the right of the nose.

Forward collision warning

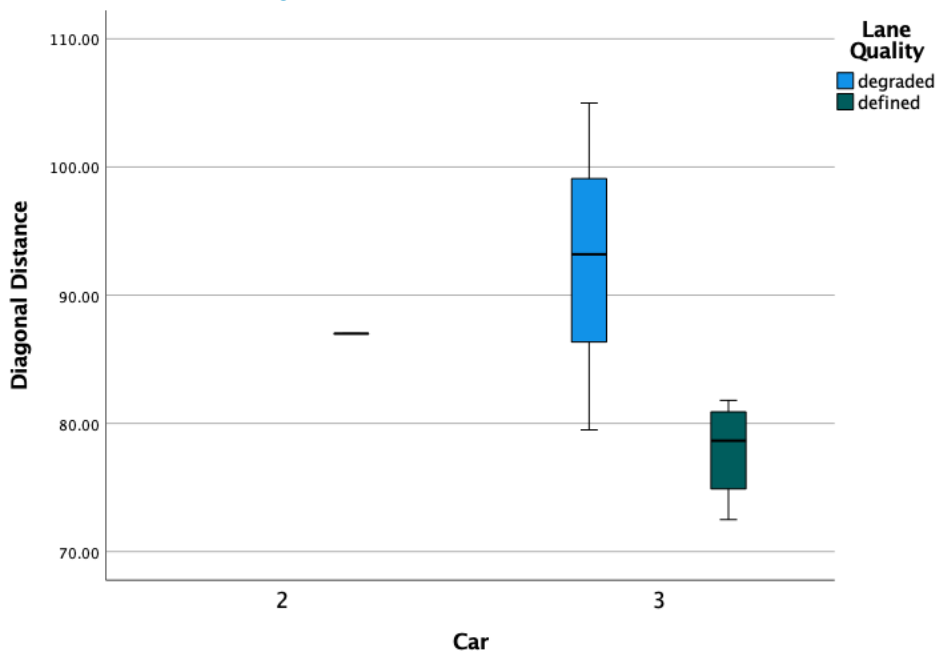


Figure 23: Diagonal distance when the forward collision warning happened

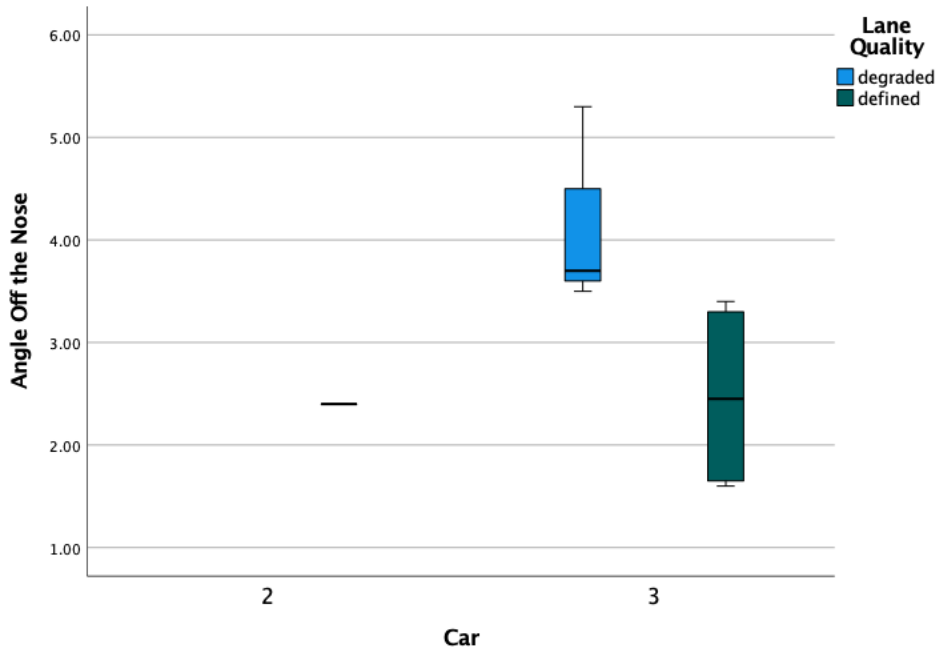


Figure 24: Angle off the nose when the forward collision warning happened

There were only Car B2 and B3 observations. The pedestrian was always to the right of the nose when a forward collision warning occurred.

Driver/Final takeover

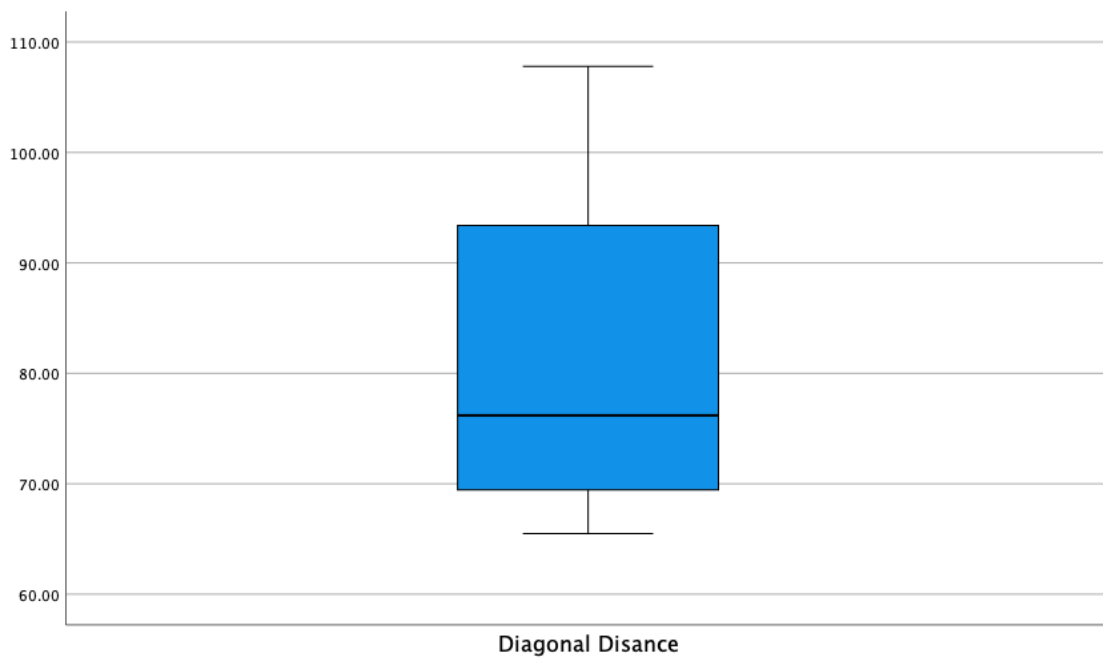


Figure 25: Diagonal distance when driver and final takeover appeared

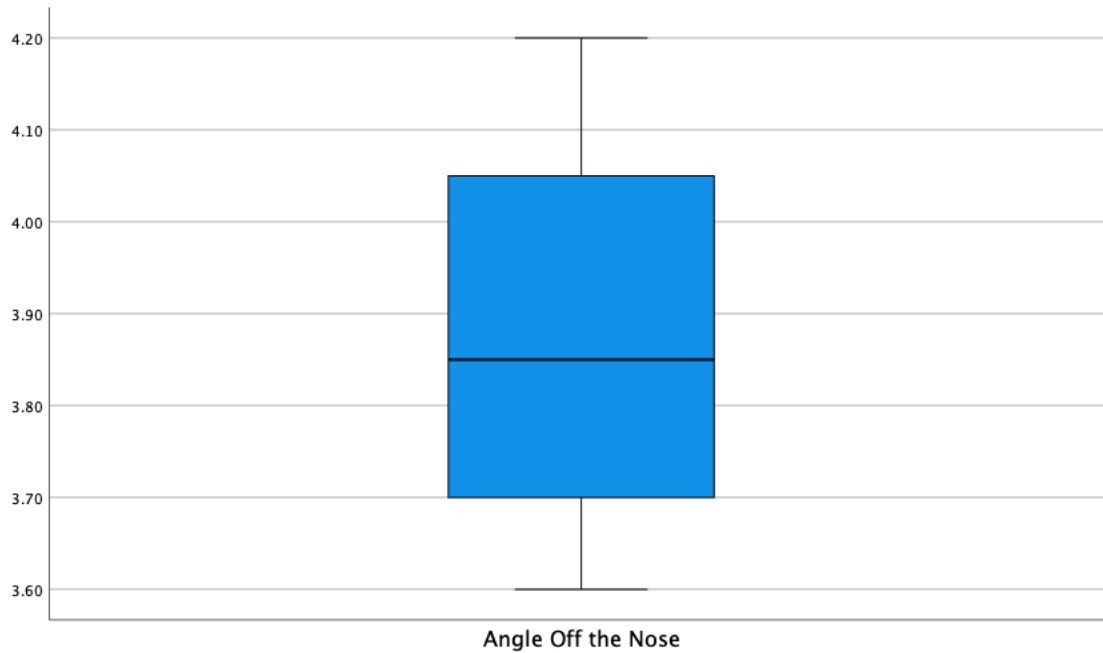


Figure 26: Angle off the nose when driver and final takeover appeared

Only Car B3 had driver and final takeover alerts, and in the degraded lanes condition. At 40 mph (59 ft/s), the forward collision warning/rapid alert/final takeover alerts happened on average 67-92 feet away, giving the pedestrian 1-1.6 seconds to clear; these were very close calls.